C. R. Chimie 5 (2002) 751–757
© 2002 Académie des sciences / Éditions scientifiques et médicales Elsevier SAS. Tous droits réservés
S1631074802014388/FLA

Structure and properties of glasses in the system $Li_2O–SnO–B_2O_3$

Akitoshi Hayashi, Miyuki Nakai, Masahiro Tatsumisago*, Tsutomu Minami

Department of Applied Materials Science, Graduate School of Engineering, Osaka Prefecture University, Sakai, Osaka 599-8531, Japan

Received 22 April 2002; accepted 6 June 2002

Abstract – Glasses in the system $Li_2O–SnO–B_2O_3$ system were prepared by a melt-quenching method. Thermal and viscous properties and local structure of these glasses were investigated. The $SnO–B_2O_3$ glasses exhibited relatively low glass-transition temperatures (T_g) around 350 °C and excellent thermal stability against crystallization. Viscosity measurements in the vicinity of T_g indicated that the glasses were considerably fragile compared to alkali borate glasses. Fraction of four-coordinated boron was maximized at the composition with 50 mol% SnO and that of nonbridging oxygen, which is not purely ionic in alkali borate systems but partially covalent, augmented with an increase in the SnO content. Correlation between glass properties and structure was discussed in the $SnO–B_2O_3$ binary system. ***To cite this article: A. Hayashi et al., C. R. Chimie 5 (2002) 751–757***
© 2002 Académie des sciences / Éditions scientifiques et médicales Elsevier SAS

borate glass / SnO based glass / glass-transition temperature / viscosity / glass structure / NMR / XPS

Résumé – Des verres de borates d'étain et de lithium ont été étudiés du point de vue des structures locales, viscosité et propriétés thermiques, révélant que ces verres sont fragiles. Les relations entre propriétés et structures sont discutées. ***Pour citer cet article : A. Hayashi et al., C. R. Chimie 5 (2002) 751–757*** © 2002 Académie des sciences / Éditions scientifiques et médicales Elsevier SAS

verres de borate / structure / propriétés thermiques

1. Introduction

Electrochemical properties of tin-oxide-based glasses have been intensively studied since 1997, when Idota et al. [1] have reported that the glasses work as anode materials for lithium secondary batteries. The electrical capacity of the glasses is over 600 mA h g^{-1}, which is almost twice as large as the capacity of graphitic carbon materials used as anodes for commercial lithium-ion secondary batteries. Although a large number of studies have been made on anode properties of tin oxide based glasses [2–7], little is known about fundamental properties such as thermal and viscous properties of the glasses. Recently, we have prepared several glasses based on SnO and indicated that the glasses exhibit not only excellent performance as anode materials but relatively low glass-transition temperatures [8]. Glasses including large amounts of PbO have been commercially used as a sealing glass because of their low softening temperature. Tin-oxide-based glasses are the most promising candidates of Pb-free low melting glasses, which are desirable from an environmental point of view [9, 10]. Glass properties are well known to closely relate to glass structure. It is thus important to investigate local structure of glasses in order to understand and improve their properties. We have analyzed glass structure of the $SnO–B_2O_3$ binary system by several spectroscopic techniques [11].

* *Correspondence and reprints.*
E-mail address: tatsu@ams.osakafu-u.ac.jp (M. Tatsumisago).

In the present study, glasses in the system Li_2O–SnO–B_2O_3 have been prepared by a conventional melt-quenching method and the glass-forming region of the system has been determined. Glass-transition temperature (T_g) and viscosity in the vicinity of T_g are systematically investigated. Local structure of the glasses is also analyzed by using solid-state NMR and X-ray photoelectron spectroscopy, and a structural model of the glasses is proposed. The correlation between glass properties and structure in the SnO–B_2O_3 binary system is discussed.

2. Experimental

The mixture of Li_2O (Kishida Chem., 99.9%), SnO (Furuuchi Chem., 99.9%), and B_2O_3 (Koujundo Chem., 99.9%) was heated in a carbon crucible at 850–1200 °C for 0.5–1 h in a dry N_2-filled glove box. The molten samples were cooled by a conventional press quenching method (the cooling rate is in the range 10^2–10^3 K s^{-1}) to yield thin disks less than 1-mm thick.

Glass-transition temperatures were determined for the samples sealed into Al pan in a dry N_2-filled glove box by a differential scanning calorimetry (DSC) (PerkinElmer, DSC 7). The heating rate was 10 °C min^{-1} in the temperature range 25–500 °C under N_2 atmosphere in all the measurements. Viscosity in the vicinity of T_g was determined using the beam-bending technique developed by Hagy et al. [12]. The measurement was performed using a thermomechanical analyzer (Mac Science, TMA-4000) to obtain activation energies E_η for viscous flow around T_g [13–15].

^{11}B MAS-NMR measurements were carried out at 96.23 MHz on a NMR spectrometer (Varian, Unity Inova 300). A pulse sequence with a single π/8 pulse was used in order to perform quantitative analysis on the spectra of quadrupolar nuclei such as ^{11}B [16, 17]. The width of a π/8 pulse length was found to be 0.7 μs for the SnO–B_2O_3 glasses. A recycle pulse delay, a spinning speed, and number of scans were respectively 2.0 s, 5 kHz, and 64–320 scans. O1s photoelectron spectroscopy was performed with an S-probe ESCA (Fions Instrument, SSX100S) using a monochromatic AlKα radiation ($h\nu$ = 1486.6 eV). Rod-shaped glass samples were fractured in an ultra-high vacuum chamber (7×10^{-8} Pa) and the generated fresh surfaces of the glasses were analyzed. In order to remove the influence of the charging effect on spectra, neutralization of the glass surface was performed during the measurement by the combined use of a low-energy flood gun and an electrically grounded nickel mesh screen placed 1 mm above the glass surface [18–20]. Calibration of the spectra was done by setting the measured binding energy of the C1s peak to 284.4 eV due to adventitious carbon accumulated in the analysis chamber of the spectrometer.

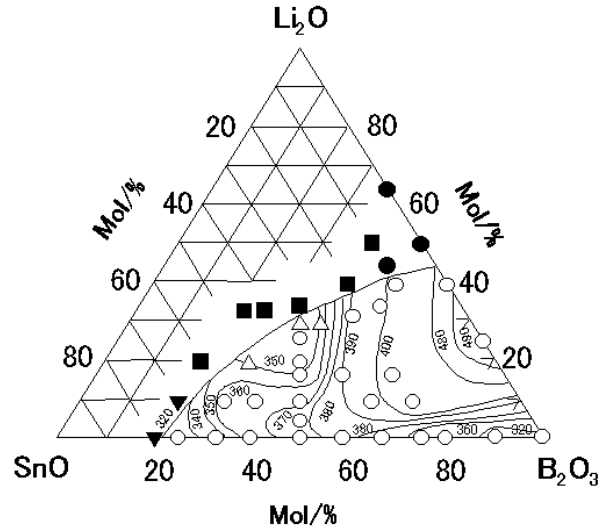

Fig. 1. Glass-forming region and glass-transition temperature isotherms (°C) in the system Li_2O–SnO–B_2O_3; ○: glass only, △: glass + traces of Sn, ▼: Sn crystals precipitated in small amounts of glass, ■: SnO crystals precipitated in small amounts of glass, and ●: $Li_2B_4O_7$ crystals precipitated in small amounts of glass.

3. Results and discussion

3.1. Glass-forming region and glass-transition temperature (T_g)

Fig. 1 shows the glass-forming region and the T_g isotherms (°C) in the system Li_2O–SnO–B_2O_3. Open circles and triangles respectively denote glassy samples and glassy samples with trace amounts of metallic Sn. The other marks denote that crystalline components were precipitated with small amounts of glasses; detailed crystalline phases are described in the caption. In the binary Li_2O–B_2O_3 system, glasses are obtained in the composition range $0 \le Li_2O$ (mol%) ≤ 40, which has been reported in a previous report [21]. Glasses are obtained in the composition range $0 \le$ SnO (mol%) ≤ 75 in the binary SnO–B_2O_3 system. The glass-forming region in the binary system with SnO is considerably wider than that in the system with Li_2O, which suggests that SnO plays the role of a network former as well as that of a network modifier. A change in the T_g isotherms in the Li_2O–SnO–B_2O_3 system is notably complicated with Li_2O and SnO contents; T_g ranges from 320 to 490 °C, which depends on a glass composition.

Fig. 2 shows the composition dependence of T_g in the SnO–B_2O_3 system. The values of T_g increase up to 40 mol% SnO and then decrease with an increase

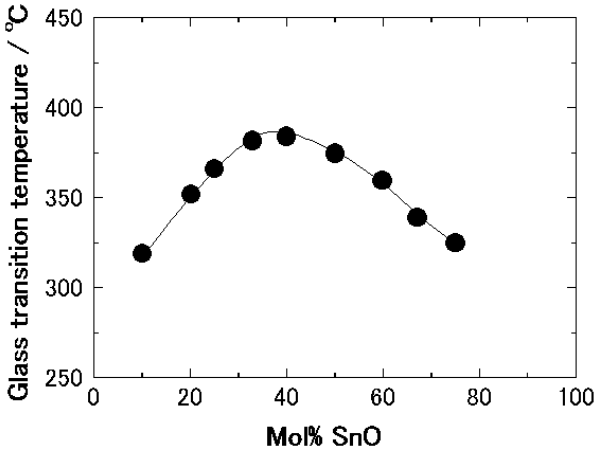

Fig. 2. Composition dependence of glass-transition temperature for the $SnO–B_2O_3$ glasses.

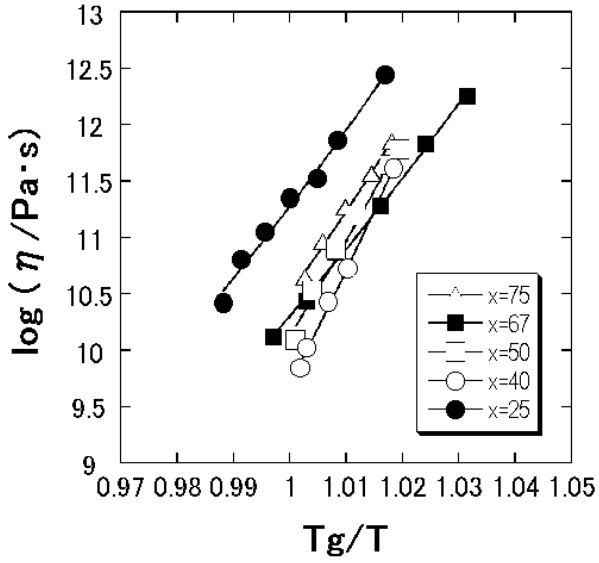

Fig. 3. Temperature dependence of viscosity in the vicinity of T_g for the x SnO·$(100 - x)$ B_2O_3 (mol%) glasses.

in the SnO content. The 40 SnO·60 B_2O_3 (mol%) glass exhibits a maximum T_g of 384 °C. A similar composition dependence of T_g was also reported in other borate glasses such as $Na_2O–B_2O_3$ [22] and $PbO–B_2O_3$ glasses [23]. The maximum T_g was 475 °C at the composition with 30 mol% Na_2O and 455 °C at the composition with 27 mol% PbO. It is revealed that T_g in the $SnO–B_2O_3$ glasses is much lower than that in the other borate glasses with Na_2O or PbO.

In the $SnO–B_2O_3$ binary system, no exothermic peaks due to crystallization were observed on DSC curves in the temperature range up to 500 °C, which suggests that the binary system with SnO has an excellent thermal stability against crystallization. In the case of an addition of Li_2O to the $SnO–B_2O_3$ system, however, an exothermic peak due to crystallization was observed in the temperature range up to 500 °C, which suggests that the addition of Li_2O lowers the thermal stability of the glasses.

3.2. Viscous properties in the vicinity of T_g

Fig. 3 shows viscosity data in the vicinity of T_g for the $SnO–B_2O_3$ glasses versus reciprocal temperatures normalized by T_g. In such a narrow temperature region, viscosity data obey the Arrhenius equation in the viscosity range 10^{10}–10^{13} Pa s. The values of E_η and E_η/T_g, where E_η is an activation energy for viscous flow in the glass-transition range, are calculated from a slope of the viscosity data.

Fig. 4 shows the composition dependence of E_η and E_η/T_g of the $SnO–B_2O_3$ glasses. The composition dependence of E_η/T_g is very similar to that of E_η. Both values of E_η and E_η/T_g g increase up to the composition with 40 mol% SnO, then decrease up to 67 mol% SnO, and increase again up to 75 mol% SnO. The maximum E_η and E_η/T_g values are respectively 1266 kJ mol^{-1} and 1.93 kJ mol^{-1} K^{-1} for the composition with 40 mol% SnO.

E_η/T_g is one of the measures of fragility of liquids; the concept of fragility has been proposed by Angell [24]. The 40 SnO·60 B_2O_3 (mol%) liquid is the most fragile in the $SnO–B_2O_3$ system. A similar composition dependence of E_η/T_g was reported in the conventional alkali borate systems such as $Na_2O–B_2O_3$ [25]. In this system, the maximum E_η/T_g value of 1.53 kJ mol^{-1} K^{-1} was obtained at the composition with 30 mol% Na_2O. The maximum value of E_η/T_g in the $SnO–B_2O_3$ system is larger than that of the

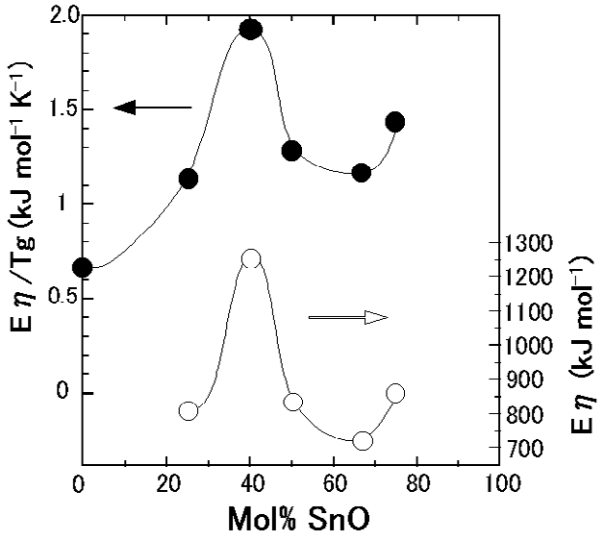

Fig. 4. Composition dependence of E_η and E_η/T_g for the $SnO–B_2O_3$ glasses.

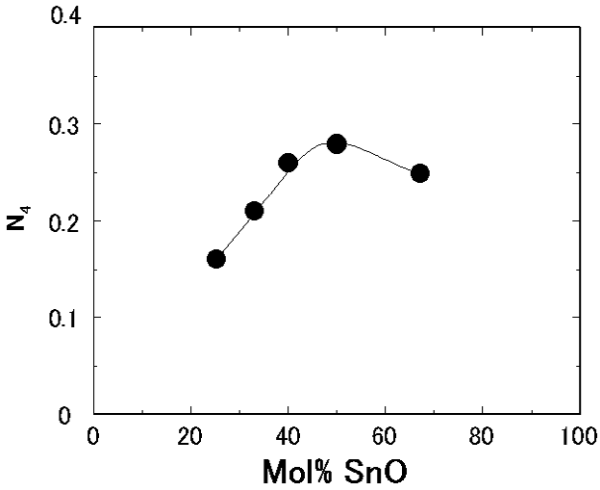

Fig. 5. Composition dependence of fraction of four-coordinated boron (N_4) for the SnO–B_2O_3 glasses.

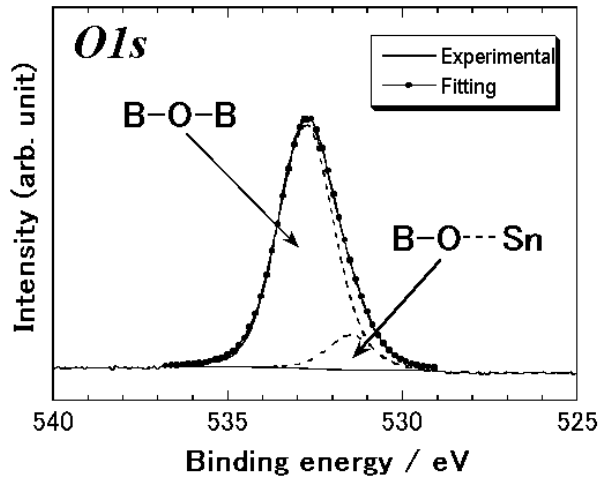

Fig. 6. O1s photoelectron spectrum of the 25 SnO·75 B_2O_3 (mol%) glass. The peak separation is also shown in this figure.

Na_2O–B_2O_3 system, suggesting that borate glasses with SnO are more fragile than alkali borate glasses.

3.3. Glass structure

^{11}B MAS-NMR measurements were performed to determine the fraction of four-coordinated boron (N_4, which means the ratio of $[BO_4]/([BO_3]+[BO_4])$) present in the SnO–B_2O_3 glasses. Fig. 5 shows the composition dependence of N_4 obtained from ^{11}B NMR spectra. It is well known that there are only BO_3 units in the pure B_2O_3 glass [17]. The BO_4 units are present at the composition with 25 mol% SnO, where N_4 is 0.16. The N_4 values increase up to 50 mol% SnO and then decrease with increasing SnO. The maximum value of N_4 is 0.28 at the composition with 50 mol% SnO.

O1s photoelectron spectroscopy was measured to investigate electronic states of oxygen in the SnO–B_2O_3 glasses. Fig. 6 shows O1s photoelectron spectrum of the 25 SnO·75 B_2O_3 (mol%) glass. The peak shape of the glass is asymmetrical; we confirmed that the peak of the glass was broadened at the lower energy side as compared with the symmetrical peak of the pure B_2O_3 glass. This broadening of the O1s peak suggests that at least two peaks are partially overlapped. A peak separation was carried out by the best-fitting program using Gaussian (70%) and Lorentzian (30%) [19, 20]; the separated peaks are also shown in Fig. 6.

In the O1s spectra of the alkali borate glasses such as the Na_2O–B_2O_3 system, two distinct peaks obviously appear; a peak at a higher energy side is assigned to bridging oxygens and the other one at a lower energy side to nonbridging oxygens [26]. We have already mentioned that the SnO–B_2O_3 system has a wide glass-forming region and four-coordinated boron is still present at compositions with high SnO content. These results suggest that SnO acts not only as a network modifier, but also as a network former. Hence, typical ionic nonbridging oxygen observed in the alkali borate glasses is not present but rather more covalent nonbridging oxygen is mainly present in the SnO–B_2O_3 glasses. Since the binding energy of the nonbridging oxygen with partial covalency is close to that of bridging oxygens, the spectrum of the SnO–B_2O_3 glass could not be clearly divided into two distinct peaks. The peak at the higher energy side in Fig. 6 is thus assigned to bridging oxygen (B–O–B) and the peak at the lower energy side to nonbridging oxygen (B–O··Sn). The component of oxygens in SnO (Sn··O··Sn) is also included probably in the peak at the lower energy side.

The relative amounts of those two kinds of oxygens were obtained from the relative areas under the two separated peaks. Fig. 7 shows the composition dependence of the relative amounts of bridging oxygen and nonbridging oxygen of the SnO–B_2O_3 glasses. Only bridging oxygens are present in the B_2O_3 glass. Addition of SnO to B_2O_3 forms nonbridging oxygens and the amounts of bridging and nonbridging oxygens are estimated to be respectively 89% and 11% at the composition with 25 mol% SnO. The amounts of nonbridging oxygens slowly increase up to the composition with 40 mol% SnO and then drastically increase with an augmentation of the SnO contents. The amounts of bridging and nonbridging oxygens are respectively 32% and 68% at the composition with 67 mol% SnO.

The structural model of the SnO–B_2O_3 glasses is proposed on the basis of the spectroscopic data mentioned above. The ^{11}B NMR measurement of the

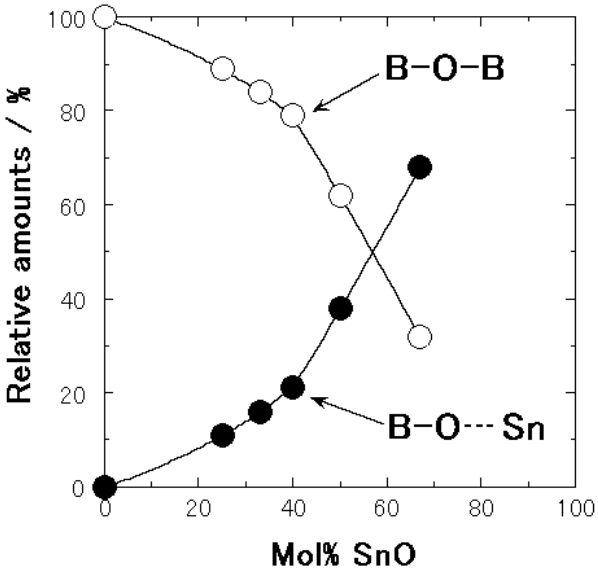

Fig. 7. Composition dependence of relative amounts of bridging oxygen (B–O–B) and nonbridging oxygen (B-O··Sn) for the $SnO–B_2O_3$ glasses.

50 $SnO{\cdot}50\ B_2O_3$ (mol%) glass revealed that the fraction of four-coordinated boron was 0.28, whereas that of three-coordinated boron was 0.72. The O1s photoelectron spectroscopy of the glass indicated that the relative amount of bridging oxygens (B–O–B) was 62%, whereas that of nonbridging oxygens (B–O··Sn) was 38%. The estimated structural model of the 50 $SnO{\cdot}50\ B_2O_3$ (mol%) glass is shown in Fig 8. The glass network consists of BO_3 (72%) and BO_4 (28%) units, and Sn(II) compensates for negative charges of BO_4 units and nonbridging oxygens.

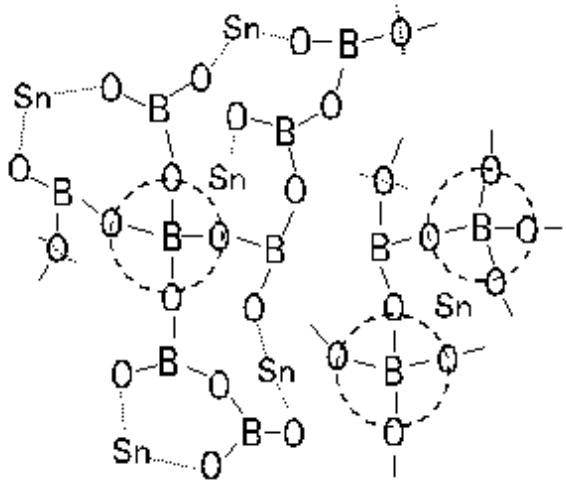

Fig. 8. Structural model of the 50 $SnO{\cdot}50\ B_2O_3$ (mol%) glass.

3.4. Correlation between glass structure and properties

The thermal and viscous properties of the $SnO–B_2O_3$ glasses are discussed from the point of view of the glass structure.

As shown in Fig. 2, the T_g values have increased up to 40 mol% SnO and then decreased with an increase in the SnO content. The composition dependence of N_4 (Fig 5) is similar to that of T_g. However, the maximum composition of T_g is different from that of N_4; the values of T_g maximize at the composition with 40 mol% SnO, whereas N_4 does with 50 mol% SnO. This difference in composition between the maximum T_g and N_4 has also been observed in the alkali borate glasses [27] and $PbO–B_2O_3$ glasses [23, 28]. The BO_4 tetrahedral units make three-dimensional network and, therefore, T_g increases with an increase in N_4. In the $SnO–B_2O_3$ glasses, the amounts of nonbridging oxygens have drastically increased for the compositions with more than 40 mol% SnO, as shown in Fig. 7. An increase in nonbridging oxygen generally lowers T_g. The maximum composition of T_g must depend on both amounts of four-coordinated boron and nonbridging oxygen in the glass structure. In this balance, T_g has maximized for the composition with 40 mol% SnO in the $SnO–B_2O_3$ glasses.

The values of E_η/T_g have maximized for the composition with 40 mol% SnO (Fig. 4) whereas N_4 maximized for the composition with 50 mol% SnO (Fig. 5). As mentioned in section 3.2, E_η/T_g is used as a measure of fragility of liquids. Lee et al. [15, 25] have reported in several borate glasses that E_η/T_g is closely linked to an average coordination number $\langle r\rangle$ of elements, which was introduced by Phillips [29] in order to explain strong glass-forming ability in chalcogenide systems. The $\langle r\rangle$ value in the $Na_2O–B_2O_3$ glasses was maximized for the composition with 30 mol% Na_2O, for which the value of E_η/T_g was also maximized [25]. The correlation between $\langle r\rangle$ and E_η/T_g was explained as follows. The $\langle r\rangle$ value of the B_2O_3 glass was calculated to be 2.40, which suggests that this glass is the most stable from the Phillips' topological point of view [29]. Since the $Na_2O–B_2O_3$ glasses, whose $\langle r\rangle$ value was larger than the 2.40 value of the B_2O_3 glass, was in the over-constrained coordination state, the glasses exhibited larger fragility [25].

We try to calculate the $\langle r\rangle$ value of the $SnO–B_2O_3$ glasses on the basis of the structural data mentioned above and discuss the correlation between $\langle r\rangle$ and E_η/T_g. In the $Na_2O–B_2O_3$ glasses [25], bonds with strong covalent character such as B–O were only taken into account and ionic bonds such as $O^-\cdot\cdot Na^+$ were neglected in the calculation of $\langle r\rangle$. On the other hand, the bond of O··Sn present in the $SnO–B_2O_3$ glasses is more covalent than the typical ionic bond

$O^{-}\cdot\cdot Na^{+}$ (see section 3.3). We have thus calculated <*r*> in extreme two manners: in a case (a), the O··Sn bond is assumed to be perfectly ionic, and, in the other case (b), the O··Sn bond is assumed to be perfectly covalent. In other words, only the B–O covalent bond is taken into account in the case (a) and both B–O and O··Sn bonds are considered in the case (b). In the case (a), the <*r*> values of the borate structural units $BO_{3/2}$, $(BO_{4/2})^{-}$, $BO_{2/2}O^{-}$, $BO_{1/2}O_2^{2-}$, and BO_3^{3-} were respectively calculated to be 2.40, 2.67, 2.00 1.71, and 1.50. In the case (b), the <*r*> values of the units $BO_{3/2}$, $BO_{4/2}Sn$, $BO_{2/2}OSn$, $BO_{1/2}O_2Sn_2$, and BO_3Sn_3 were respectively 2.40, 3.14, 2.22, 2.15, and 2.12; the coordination number of Sn was assumed to be 6 in the $BO_{4/2}Sn$ unit and 2 in the other units.

The composition dependence of <*r*> calculated for the SnO–B_2O_3 glasses is shown in Fig. 9. Open and closed circles denote the <*r*> values in the cases (a) and (b), respectively. The <*r*> value of pure B_2O_3 glass is 2.40. The <*r*> value calculated in the case (a) slowly decreases up to the composition with 40 mol% SnO and then drastically decreases with an increase in the SnO content. On the other hand, the <*r*> value calculated in the case (b) increases up to the composition with 40 mol% SnO and then decreases. The proper <*r*> value of the SnO–B_2O_3 glasses must be an intermediate value between the extreme two cases of (a) and (b), and hence <*r*> is presumed to be maximized at the composition with 40 mol% SnO. This suggests that the composition dependence of <*r*> is closely related with that of fragility with E_η/T_g in the SnO–B_2O_3 system.

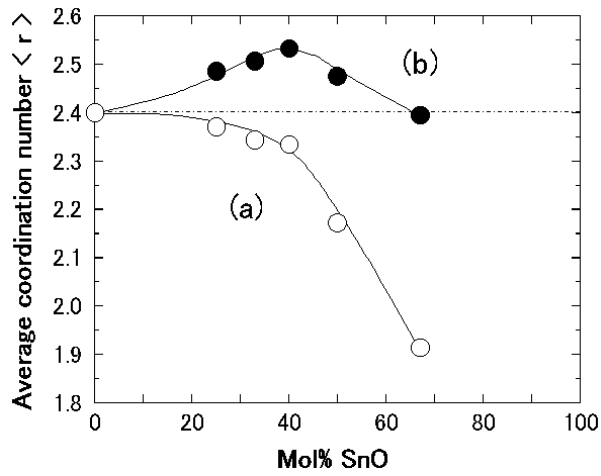

Fig. 9. Composition dependence of average coordination number <*r*> for the SnO–B_2O_3 glasses. The calculation of <*r*> was carried out in two manners: in the first case (a), the O··Sn bond was assumed to be perfectly ionic, and in the other case (b), the O··Sn bond was assumed to be perfectly covalent. See text for details.

4. Conclusions

Glasses in the system Li_2O–SnO–B_2O_3 were prepared by a conventional melt-quenching method. The glass-forming region of the SnO–B_2O_3 system was $0 \le$ SnO (mol%) ≤ 75, which region was considerably wider than that of the Li_2O–B_2O_3 system ($0 \le Li_2O$ (mol%) ≤ 40). The SnO–B_2O_3 glasses showed relatively low glass-transition temperature (T_g) around 350 °C and excellent thermal stability against crystallization, which suggests that these glasses are one of the most promising Pb-free low melting glasses. On the other hand, an addition of Li_2O to the glasses lowered thermal stability. Both values of T_g and E_η/T_g were maximized at the composition with 40 mol% SnO in the SnO–B_2O_3 system. In particular, it is noteworthy that the 40 SnO·60 B_2O_3 (mol%) glass with a large E_η/T_g of 1.93 kJ mol^{-1} K^{-1} is considerably fragile compared to other oxide glasses.

^{11}B MAS NMR measurements indicated that the fraction of four-coordinated boron was maximized at the composition with 50 mol% SnO. It was revealed from O1s photoelectron spectra that an addition of small amounts of SnO formed nonbridging oxygen, which is not purely ionic in alkali borate systems but partially covalent in the SnO–B_2O_3 system. The amounts of nonbridging oxygen gradually increased in the range SnO ≤ 40 mol% and then drastically increased in the range SnO > 40 mol%, with an increase in the SnO content.

The correlation between glass properties and structure in the SnO–B_2O_3 system was discussed. The composition dependence of T_g was expected to be influenced by the fraction of not only four-coordinated boron but also nonbridging oxygen. We also explained the composition dependence of E_η/T_g in terms of the calculated average coordination number <*r*>.

Acknowledgements. This work was supported by the Grand-in-Aid for Scientific Research on Priority Areas (B) and Section (B) from the Ministry of Education, Culture, Sports, Science and technology of Japan, and by Research Fellowships of the Japan Society for the Promotion of Science for Young Scientists.

References

[1] Y. Idota, T. Kubota, A. Matsufuji, T. Miyasaka, Science 276 (1997) 1395.

[2] I.A. Courtney, J.R. Dahn, J. Electrochem. Soc. 144 (1997) 2943.

[3] I.A. Courtney, R.A. Dunlap, J.R. Dahn, Electrochim. Acta 45 (1999) 51.

[4] Y.W. Xiao, J.Y. Lee, A.S. Yu, Z.L. Liu, J. Electrochem. Soc. 146 (1999) 3623.

[5] S. Machill, T. Shodai, Y. Sakurai, J. Yamaki, J. Solid State Electrochem. 3 (1999) 97.

[6] G.R. Goward, L.F. Nazar, W.P. Power, J. Mater. Chem. 10 (2000) 1241.

[7] J.Y. Lee, Y.W. Xiao, Z.L. Liu, Solid State Ionics 133 (2000) 25.

[8] M. Nakai, A. Hayashi, H. Morimoto, M. Tatsumisago, T. Minami, J. Ceram. Soc. Jpn 109 (2001) 1010.

[9] P.Y. Shih, S.W. Yung, T.S. Chin, J. Non-Cryst. Solids 224 (1998) 143.

[10] K. Morinaga, S. Fujino, J. Non-Cryst. Solids 282 (2001) 118.

[11] A. Hayashi, M. Nakai, M. Tatsumisago, T. Minami, Y. Himei, Y. Miura, M. Katada, J. Non-Cryst. Solids 306 (2002) 227.

[12] H.E. Hagy, J. Am Ceram. Soc. 46 (1963) 93.

[13] M. Tatsumisago, B.L. Halfpap, L. Green, S.M. Lindsay, C.A. Angell, Phys. Rev. Lett. 64 (1990) 154.

[14] S.K. Lee, M. Tatsumisago, T. Minami, J. Ceram. Soc. Jpn 101 (1993) 1018.

[15] S.K. Lee, M. Tatsumisago, T. Minami, Phys. Chem. Glasses 38 (1997) 144.

[16] F. Taulelle, C. Bessada, D. Massiot, J. Chem. Phys. 89 (1992) 379.

[17] J.A. Sills, S.W. Martin, D.R. Torgeson, J. Non-Cryst. Solids 168 (1994) 86.

[18] Y. Himei, Y. Miura, T. Nanba, A. Osaka, J. Non-Cryst. Solids 211 (1997) 64.

[19] A. Hayashi, M. Tatsumisago, T. Minami, Y. Miura, J. Am. Ceram. Soc. 81 (1998) 1305.

[20] A. Hayashi, M. Tatsumisago, T. Minami, Y. Miura, Phys. Chem. Glasses 39 (1998) 145.

[21] M. Tatsumisago, T. Minami, Mater. Chem. Phys. 18 (1987) 1.

[22] J.E. Shelby, J. Am. Ceram. Soc. 66 (1983) 225.

[23] A.M. Zahra, C.Y. Zahra, B. Piriou, J. Non-Cryst. Solids 155 (1993) 45.

[24] C.A. Angell, J. Non-Cryst. Solids 73 (1985) 1.

[25] S.K. Lee, M. Tatsumisago, T. Minami, J. Ceram. Soc. Jpn 103 (1995) 398.

[26] S. Matsumoto, Y. Miura, C. Murakami, T. Nanba, Proc. 2nd Int. Conf. on Borate Glasses, Crystals and Melts, Abingdon, 1997, p. 173.

[27] G.D. Chryssikos, E.I. Kamistsos, M.A. Karakassides, Phys. Chem. Glasses 31 (1990) 109.

[28] P.J. Bray, M. Leventhal, H.O. Hooper, Phys. Chem. Glasses 4 (1963) 47.

[29] J.C. Phillips, J. Non-Cryst. Solids 34 (1979) 153.